Since January 2020 Elsevier has created a COVID-19 resource centre with free information in English and Mandarin on the novel coronavirus COVID-19. The COVID-19 resource centre is hosted on Elsevier Connect, the company's public news and information website.

Analytica Chimica Acta 1208 (2022) 339846

Contents lists available at ScienceDirect

Analytica Chimica Acta

journal homepage: www.elsevier.com/locate/aca

Target-triggered cascade signal amplification for sensitive electrochemical detection of SARS-CoV-2 with clinical application

Ying Deng [a], Ying Peng [a], Lei Wang [a], Minghui Wang [a], Tianci Zhou [a], Liangliang Xiang [b], Jinlong Li [b,*], Jie Yang [a], Genxi Li [a,c,**]

[a] State Key Laboratory of Analytical Chemistry for Life Science, School of Life Sciences, Nanjing University, Nanjing, 210023, PR China
[b] The Second Hospital of Nanjing, Nanjing University of Chinese Medicine, Nanjing, 210003, PR China
[c] Center for Molecular Recognition and Biosensing, School of Life Sciences, Shanghai University, Shanghai, 200444, PR China

ARTICLE INFO

Keywords:
SARS-CoV-2 RNA
COVID-19
Cascade signal amplification
Electrochemical biosensor

ABSTRACT

The spread of severe acute respiratory syndrome coronavirus 2 (SARS-CoV-2) has led to the outbreak of the 2019 coronavirus (COVID-19) disease, which greatly challenges the global economy and health. Simple and sensitive diagnosis of COVID-19 at the early stage is important to prevent the spread of pandemics. Herein, we have proposed a target-triggered cascade signal amplification in this work for sensitive analysis of SARS-CoV-2 RNA. Specifically, the presence of SARS-CoV-2 RNA can trigger the catalytic hairpin assembly to generate plenty of DNA duplexes with free 3′-OH termini, which can be recognized and catalyzed by the terminal deoxynucleotidyl transferase (TdT) to generate long strand DNA. The prolonged DNA can absorb substantial $Ru(NH_3)_6^{3+}$ molecules via electrostatic interaction and produce an enhanced current response. The incorporation of catalytic hairpin assembly and TdT-mediated polymerization effectively lowers the detection limit to 45 fM, with a wide linear range from 0.1 pM to 3000 pM. Moreover, the proposed strategy possesses excellent selectivity to distinguish target RNA with single-base mismatched, three-base mismatched, and random sequences. Notably, the proposed electrochemical biosensor can be applied to analyze targets in complex circumstances containing 10% saliva, which implies its high stability and anti-interference. Moreover, the proposed strategy has been successfully applied to SARS CoV-2 RNA detection in clinical samples and may have the potential to be cultivated as an effective tool for COVID-19 diagnosis.

1. Introduction

The outbreak of coronavirus disease 2019 (COVID-19) aroused by severe acute respiratory syndrome coronavirus 2 (SARS-CoV-2) has caused large-scale infections and deaths, posing a significant threat to global healthcare systems [1]. Although the mortality has been largely controlled due to the popularization of vaccines and extensive experience of medical staff, SARS-CoV-2 continues its prevalence due to its high contagiousness [2,3]. Coordinating accurate diagnosis, timely isolation, and appropriate therapy is an effective method to control the pandemic. Among them, proper diagnosis using sensitive, conveniently-operated, and accessible technologies is the premise for isolation and therapy [4,5]. Quantitative reverse transcription polymerase chain reaction (qRT-PCR) has been recognized as the current gold standard for SARS-CoV-2 detection for its robust analytical performance [6–8]. However, it meets some technical drawbacks, such as long assay time, high-cost instruments, and involvement of trained personnel. Moreover, some studies have revealed that qRT-PCR analysis may provide false-negative results, and many patients are not diagnosed until multiple repeated swab sampling and detection [9,10]. Therefore, it is still in urgent need to solve the current dilemma by proposing sensitive and selective methods for SARS-CoV-2 detection.

As a kind of viable alternative method for the diagnosis, many biosensor-based assays for SARS-CoV-2 detection have been proposed, such as colorimetric biosensors [11,12], fluorescent biosensors [13,14], localized surface plasmon resonance (LSPR) based biosensors [15,16], electrochemical biosensors [2,4], etc. Among these, electrochemical biosensors have provided an alternative way for viruses detection due to the advantages of rapid response, low-cost instruments, convenient operation, user-friendlliness, and suitable for miniaturization [17–20].

* Corresponding author.
** Corresponding author. State Key Laboratory of Analytical Chemistry for Life Science, School of Life Sciences, Nanjing University, Nanjing, 210023, PR China.
E-mail addresses: jinlonglilab@njucm.edu.cn (J. Li), genxili@nju.edu.cn (G. Li).

https://doi.org/10.1016/j.aca.2022.339846
Received 26 March 2022; Received in revised form 14 April 2022; Accepted 16 April 2022
Available online 20 April 2022
0003-2670/

For example, we have designed an electrochemical biosensor for the detection of SARS-CoV-2 spike S1 protein via an aptamer-functionalized biomimetic nanochannel, which can rapidly detect the SARS-CoV-2 viral particles in one step without other reagents [2]. Song et al. [21] have proposed an antifouling electrochemical biosensor for SARS-CoV-2 detection by introducing the polymerized polyaniline nanowires and elaborate designed inverted Y-peptides, which can successfully detect SARS-CoV-2 at a low concentration of 3.5 fM. Lu et al. [22] have integrated the loop probe-mediated isothermal amplification strategy with electrochemical technology to analyze the SARS-CoV-2 in one-pot to avoid cross-contamination, which realizes fast readout within 30–40 min, with an ultra-low detection limit of 1 copy/μL. Nonetheless, among these methods, the cost and convenience may be sacrificed because of either the involvement of the design of probes modified with additional electroactive labels or the complex synthesis procedure of nanomaterials.

Catalytic hairpin assembly (CHA), a typical non-enzymatic nucleic acid circuit, has been deemed as a high-sensitivity tool for signal amplification with low background [23–26], which is suitable for the detection and quantification of nucleic acids target [27]. In this paper, we report a target-triggered cascade signal amplification strategy for the SARS-CoV-2 Rdrp gene detection via integrating the CHA and extraordinary polymerization ability of terminal deoxynucleotidyl transferase (TdT). TdT is a kind of template-free DNA polymerase which is able to elongate the single strand DNA by catalyzing the addition of deoxynucleotides to the free 3′ termini of DNA [28]. In this work, the well-designed hairpins are modified on the gold electrode via forming an Au–S bond on the 3-termini, so it is unable to be extended by the TdT. In the presence of the SARS-CoV-2 RNA, the CHA reaction can proceed successfully to generate a large number of DNA duplexes with free 3' –OH termini on the electrode surface. With the addition of TdT, DNA strands can be polymerized and generate long strands to absorb the electrochemical molecules, $Ru(NH_3)_6^{3+}$. So, an electrochemical biosensor can be fabricated for the sensitive assay of SARS-CoV-2 RNA. The proposed biosensor has also been applied for the detection of SARS-CoV-2 RNA in clinical samples and succeeded in distinguishing COVID-19 patients from normal individuals.

2. Experimental section

2.1. Materials

All customized DNA strands used in this research were synthesized and purified by Invitrogen Biotechnology Co, Ltd. (Shanghai, China). The oligonucleotides sequences were designed by ourselves with the assistance of Nucleic Acid Package (NUPACK), and the sequences were listed in Table S1. The terminal deoxynucleotidyl transferase (TdT) enzyme and deoxyribonucleotides mixture (dNTPs) were purchased from Beyotime Biotechnology (Shanghai, China). Hexaamminerruthenium (III) chloride ($Ru(NH_3)_6Cl_3$) was ordered from Solarbio Life Sciences Co., Ltd (Beijing, China). 6-Mercapto-1-hexanol (MCH), N,N,N′,N′-Tetramethylethylenediamine (TEMED), ammonium persulfate (APS), and Tris(2-carboxyethyl)phosphine hydrochloride (TCEP) were supplied by Sigma-Aldrich (Shanghai, China). All reagents were of analytical grades. The experimental water was purified by a Millipore water purification system.

2.2. Preparation of the modified electrodes

The Au electrode was pretreated in accordance with the previous protocol with modification [29]. Firstly, the Au electrode was successively polished with alumina powder of 1.0 μm, 0.3 μm, and 0.05 μm, and then sonicated in ethanol and distilled water for 5 min. Next, the Au electrode was immersed in piranha solution (H_2SO_4: H_2O_2 = 3:1, v/v) for 30 min. Subsequently, the Au electrode was electrochemically cleaned in 0.5 M H_2SO_4 solution until a stable cyclic voltammetry curve appeared. After being rinsed with distilled water and dried with nitrogen, a clean Au electrode with a mirror-like surface was prepared. Before immobilization on the prepared Au electrode surface, the HP1 was treated with 10 mM TCEP to reduce the S–S bonds. Then 10 μL of DNA immobilization solution (10 mM Tris-HCl, 1.0 mM EDTA, and 1.0 M NaCl, pH 7.4) containing 0.5 μM HP1 was dropped on the electrode and incubated for 2 h at 37 °C, followed by incubating with 1 mM MCH solution for 30 min at 37 °C to avoid the nonspecific adsorption.

2.3. SARS-CoV-2 RNA detection

Firstly, 10 μL of hybridization buffer containing 0.5 μM HP2 and target were added to the electrode and incubated for 2 h at 37 °C. After rinsing three times with distilled water, 10 μL of the mixture of dNTP (1 mM), TdT (10 U), and TdT reaction buffer were added and incubated for 1 h at 37 °C. Finally, the electrode was immersed in 5 mL 10 mM Tris-HCl buffer containing 5 μM $Ru(NH_3)_6^{3+}$ for 15 min and ready for the following electrochemical detection.

2.4. Electrochemical measurements

Electrochemical impedance spectra (EIS) and differential pulse voltammetry (DPV) measurements were performed on a CHI660C electrochemical workstation (CH Instruments, USA) with a three-electrode system. EIS was measured in solution including 5 mM $[Fe(CN)_6]^{3-/4-}$ and 1 M KCl and DPV was carried out in 10 mM Tris-HCl buffer containing 5 μM $Ru(NH_3)_6^{3+}$. The detailed parameter settings are as follows: bias potential, 0.224 V; amplitude, 5 mV; frequency range, 0.1 Hz to 10 kHz for EIS, amplitude, 50 mV; pulse width, 0.05 s; scan range 0 to −0.45 V for DPV.

2.5. Clinical sample analysis

For the laboratory testing, the clinical samples were collected and provided by the Second Hospital of Nanjing. The research was approved by the scientific ethical committee of the Second Hospital of Nanjing and Nanjing University (Project Number: 2020-LS-ky003), and informed consent was obtained in all cases. Total RNA was extracted from the oropharyngeal swab samples with a Nucleic Acid Isolation Kit (Magnetic Beads) from Bioperfectus Technologies (Taizhou, China) in accordance with the instructions and then stored in −80 °C for further use. Taking1 μL of extracted RNA for further analysis according to the above-mentioned protocol.

2.6. Electrophoresis experiment

The 10% polyacrylamide gel electrophoresis (PAGE) is conducted in 1 × TBE buffer, 10% APS and TEMED. For the analysis of the feasibility of CHA, 1 μM HP1 and HP2 are incubated with or without 100 nM target DNA for 2 h at 37 °C. Thereafter, the above samples are injected into 10% PAGE and conducted for 60 min at 100 V. Finally, the gel electrophoresis image is observed through Gel Imaging System.

3. Results and discussion

3.1. Principle of the proposed biosensor

Scheme 1 illustrates the mechanism of the target-triggered cascade signal amplification for electrochemical assay of SARS-CoV-2 RNA. We have selected a 26-nucleotide sequence from the SARS-CoV-2 RdRp gene located in the ORF1ab region as the target [15], which can distinguish SARS-CoV-2 from other coronaviruses with high specificity [30,31]. The designed hairpin HP1 and HP2, which exist complementary sequences, can maintain independent stable structures separately, because their complementary sequences are blocked in their stems, respectively. Firstly, the HP1 containing a thiol group at the 3′-termini has been

assembled on the electrode as a sensing layer by forming the Au–S bond. In this state, TdT-induced DNA polymerization cannot be initiated on the electrode surface because of the lack of free 3′-OH termini, thus only a low signal can be detected. However, after addition of target RNA, the RNA sequence can hybridize with the exposed toehold domain (6-base) of HP1 and generate the H1/RNA duplex by initiating the first branch migration, accompanied with the exposure of the other single-stranded toehold domain (8-base), which can further hybridize with HP2. Then, the second branch migration reaction is successfully initiated to form the HP1/HP2 duplex, along with the release of the target. The free target can circularly unfold another HP1 and trigger the multicycle hybridization between HP1 and HP2, producing amounts of HP1/HP2 duplexes on the electrode. Moreover, the surface-hybridized HP2 with free 3′-OH can be recognized by TdT enzyme to generate long-strand DNA in a dNTP pool. Consequently, a large number of electrochemical signal molecules, Ru $(NH_3)_6^{3+}$ can be attached to the negatively charged phosphate backbone of DNA through electrostatic interaction. Therefore, in the presence of a small amount of target RNA, many HP1/HP2 duplexes can be generated to introduce numerous $Ru(NH_3)_6^{3+}$ into the sensing system and obtain a significantly enhanced electrochemical signal for the detection of SARS-CoV-2.

3.2. Feasibility verification of the principle

We have first verified the feasibility of target induced assembly of the probe duplexes (HP1/HP2) via gel electrophoresis experiment. As a proof-of-concept, the hybridization reaction between capture probe HP1 and catalytic probe HP2 has been blocked in the absence of the target, implying the stable hairpin structures of HP1 and HP2 (Fig. S1, lane 4). After the addition of the target, a distinct band of HP1/HP2 duplexes appears (lane 5), along with the band of HP1 (lane 2) and HP2 (lane 3) weakening, which confirms the target triggered catalytic assembly of HP1 and HP2. Then, the stepwise modification of the working electrode has been investigated by electrochemical impedance spectroscopy (EIS) with $[Fe(CN)_6]^{3-/4-}$ redox couple. As depicted in Fig. 1A, the bare Au electrode shows almost a straight line (curve a) indicating a low electron transfer resistance. After modifying with HP1 and MCH, a semicircle appears (curve b), which can be explained by the hindering effect of negatively charged phosphate skeleton on interfacial electron transfer. The semicircular diameter increases with the addition of the target RNA and HP2 (curve c), indicating that the CHA reaction is successfully triggered and resulting HP1/HP2 duplexes enhance electronegativity and steric hindrance. Moreover, a larger diameter is observed with the addition of TdT, since the free 3′-OH of HP2 can be catalyzed by TdT and generates a long single strand, which may further hinder the electron transfer on the electrode. Afterward, differential pulse voltammetry (DPV) has been applied to investigate the feasibility of the proposed biosensor. As illustrated in Fig. 1B, a low electrochemical response is observed without SARS-CoV-2 RNA (curve a). However, in the presence of the SARS-CoV-2 RNA (curve b), the current increases since the target can trigger the CHA reaction. Moreover, the incubation of TdT leads to a further enhancement of the electrochemical response (curve c), demonstrating TdT-induced polymerization for signal amplification. The results confirm the combination of CHA and TdT can achieve better performance for SARS-CoV-2 detection.

3.3. Optimization of experimental conditions

To achieve the best performance for SARS-CoV-2 RNA detection, some experimental parameters should be optimized. First, the incubation concentration of HP1 on the gold electrode has been optimized. As shown in Fig. S2A, the current response gradually enhances as the concentration of HP1 increases from 0.1 μM to 0.5 μM and arrives at a plateau thereafter. So, 0.5 μM has been selected as the optimal concentration of HP1. Then, the influence of the reaction time of CHA has been investigated. As depicted in Fig. S2B, with the extension of the reaction time, the current increases continuously and almost reaches a platform at 120 min. Therefore, 120 min has been selected as the best reaction time in the subsequent research. TdT reaction time may also affect the efficiency of the proposed method by affecting the length of single-strand DNA. So, the effect of TdT reaction time has also been investigated by gradually prolonging the incubation time. In Fig. S2C, with the augment of reaction time, the current increases and reaches a steady-state at the time of 60 min, which can be ascribed to the fact that the growing single-strand DNA may form secondary structures to hinder the catalysis of TdT [32]. Thus, 60 min is sufficient for the preparation of proposed biosensor.

3.4. Analytical performances

With the optimal experimental conditions, the efficiency of the proposed biosensor in Rdrp gene quantification has been further studied by recording the DPV signals. Fig. 2A reveals the changes in current intensity in responding to the different concentrations of SARS-CoV-2 RNA. The current intensity enhances with the increased concentration of the target in the range from 0.1 pM to 3000 pM. Fig. 2B illustrates a linear relationship between DPV signals and the logarithm of the SARS-CoV-2 RNA concentration. The correlation equation is I (μA) = 1.462 lgc

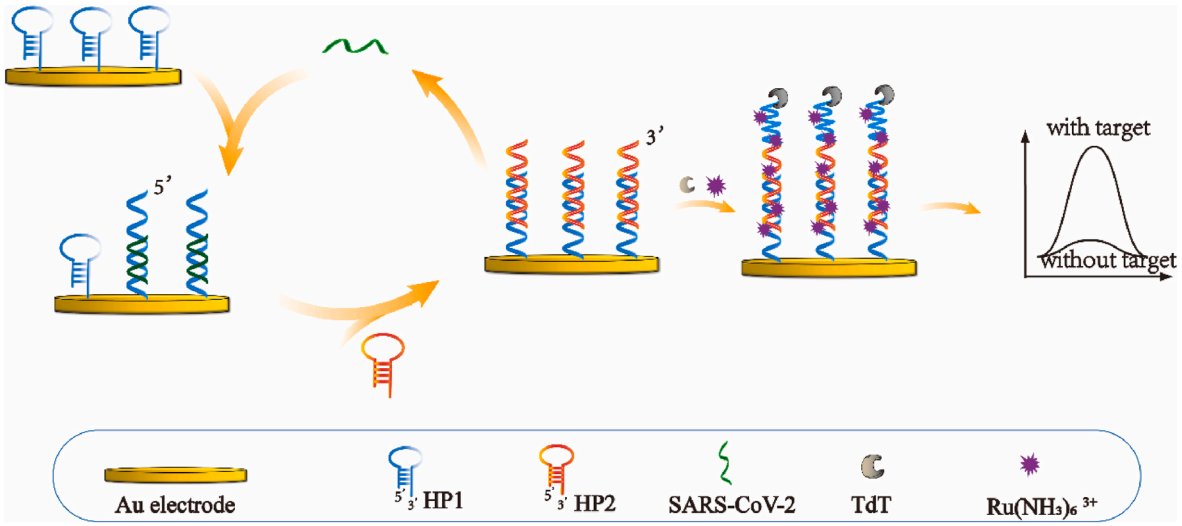

Scheme 1. Schematic diagram of the target-triggered signal amplification for sensitive electrochemical detection of SARS-CoV-2 RNA.

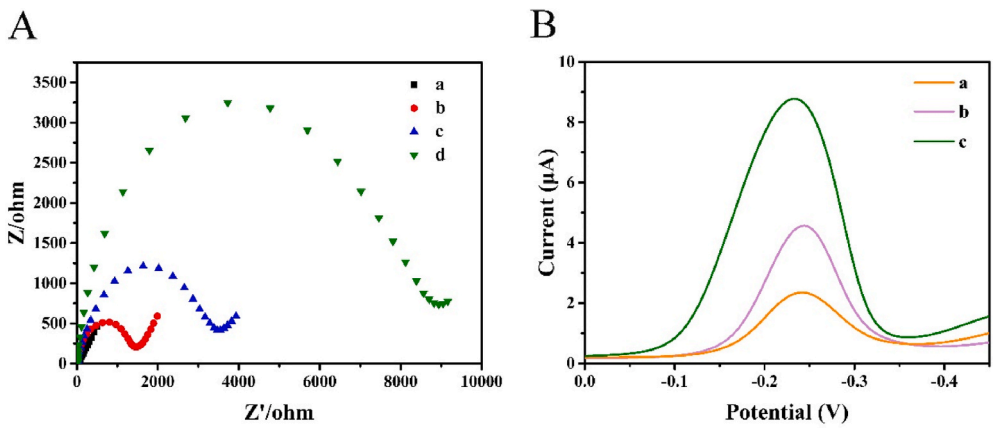

Fig. 1. (A) EIS measurements corresponding to the stepwise treatment of Au electrode. (a) bare Au electrode, (b) MCH/HP1/Au, (c) (HP2+target)/MCH/HP1/Au, (d) (TdT + HP2+target)/MCH/HP1/Au. (B) DPV signals under different reaction conditions: (a) TdT/MCH/HP1/Au incubated with $Ru(NH_3)_6^{3+}$, (b) (HP2+target)/MCH/HP1/Au incubated with $Ru(NH_3)_6^{3+}$, (c) (TdT + HP2+target)/MCH/HP1/Au incubated with $Ru(NH_3)_6^{3+}$. The concentration of the target RNA is 1 nM.

(pM) - 0.669 ($R^2 = 0.997$) and the limit of detection (LOD) is calculated to be 45 fM according to 3σ rule, i.e., LOD = 3σ/k, where σ is the standard deviation of the blank, and k is the slope of the calibration plot. So, the LOD achieved in this work is better than other recently reported methods (Table S2). Moreover, we have further investigated the specificity by measuring the current signals in response to three irrelevant sequences including a single-base mismatched (SM) sequence, a three-base mismatched (TM) sequence, and a random sequence. As shown in Fig. 3A, the lower DPV signal is observed in responding to 500 pM random sequence group and the control group. Although the currents generated by the TM group and SM group are slightly higher, they are still far lower than that of the target group. The results indicate that the proposed biosensor has excellent selectivity towards SARS-CoV-2 RNA. Moreover, the relative standard deviation (RSD) is calculated as 1.52% by conducting six independent experiments for the detection of SARS-CoV-2 RNA at the concentration of 1000 pM, indicating remarkable reproducibility of the proposed method.

3.5. *Analytical performance in complex environment and clinical samples*

To investigate the analytical performance of the proposed electrochemical biosensor in complex biological circumstances, the SARS-CoV-2 RNA spiked in 10% saliva are tested to compare with those spiked in Tris-HCl. For the same concentration target, the current intensity in 10% saliva is almost the same as that in Tris-HCl, showing the stability and anti-interference of this biosensor in complex environment (Fig. 3B).

Thereafter, we have verified the analytical performance of the proposed biosensor on clinical specimens. In brief, isolation RNA from oropharyngeal swabs of five healthy individuals and five COVID-19 patients for further test. As revealed in Fig. 4A, the measured current from the COVID-19 patient group is significantly higher than that from the healthy group. Additionally, the result of the scatterplot in Fig. 4B shows a distinguished difference between the COVID-19 patients and healthy individuals, demonstrating the potential clinical application of our method.

4. Conclusion

Overall, we have proposed a sensitive and conveniently-operated electrochemical biosensor for the detection of SARS-CoV-2 based on the help of the target-triggered cascade signal amplification strategy. In the proposed biosensor, the target sequence can serve as an efficient trigger for the following self-assembly reaction of the auxiliary hairpins, in which free 3′-OH can be introduced to the formed double-stranded DNA. Then, the DNA elongation mediated by TdT can lead to significantly amplified signals. Thus, the biosensor shows high sensitivity for SARS-CoV-2 RNA detection and realizes a low detection limit of 45 fM. Moreover, the proposed method possesses excellent selectivity, good reproducibility, and high resistance in complex environments. It has also been successfully applied for the detection of SARS-CoV-2 RNA from the

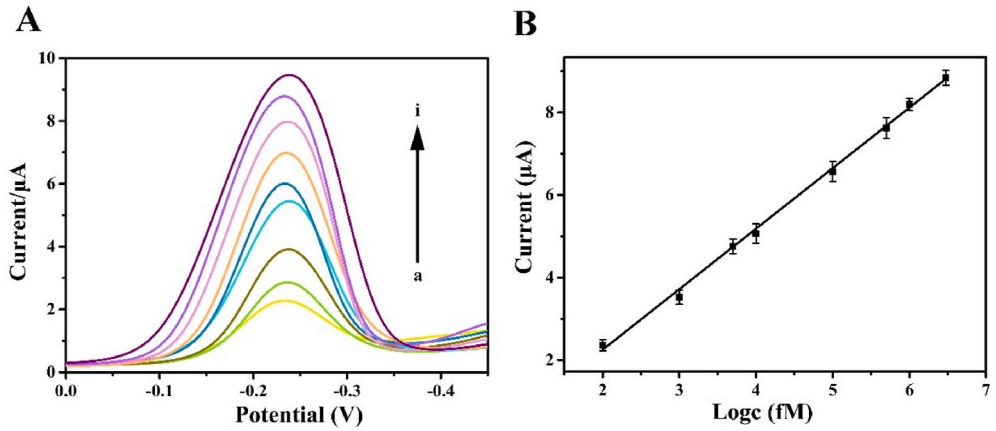

Fig. 2. The quantitative analysis for the detection of SARS-CoV-2 RNA. (A) The DPV signals corresponding to SARS-CoV-2 RNA with different concentrations. a–i: 0, 0.1, 1, 5, 10, 100, 500, 1000, 3000 pM, respectively. (B) Linear relationship between the DPV signals and the logarithm of SARS-CoV-2 RNA concentration. Error bars indicate standard deviations (n = 3).

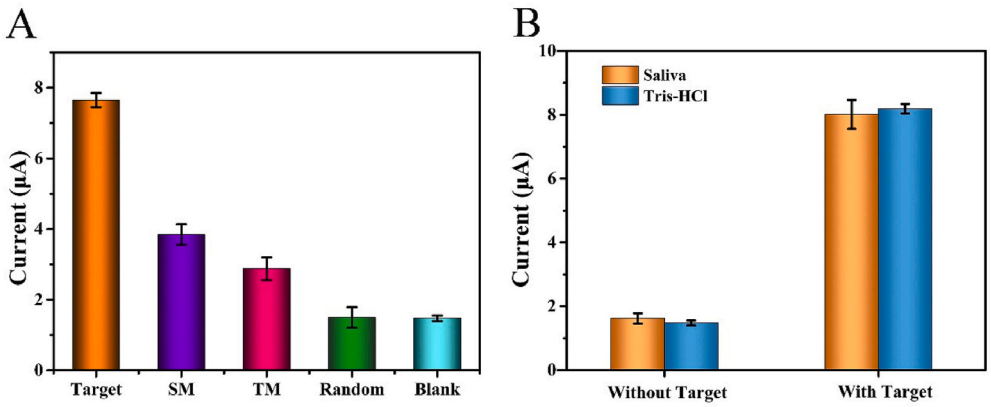

Fig. 3. (A) Selectivity of the proposed biosensor. SM represents for single-base mismatched sequence, TM represents for three-base mismatched sequence. The concentration of the analyte is 500 pM. (B) Analytical performance in Tris-HCl and 10% saliva without or with SARS-CoV-2. The concentration of the target is 1000 pM. Error bars indicate standard deviations (n = 3).

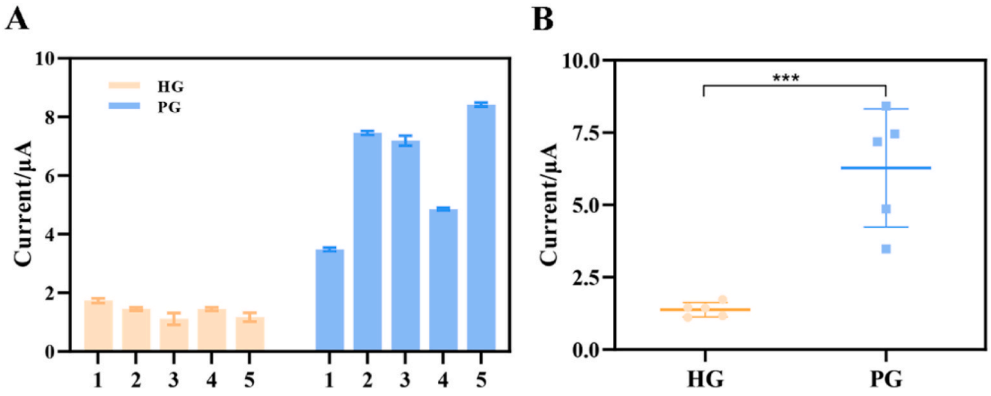

Fig. 4. (A) DPV responses of the clinical specimens collected from healthy group (HG) and patient group (PG). (B) Scatterplot of the clinical specimens of HG and PG. (***, $p < 0.001$). Error bars indicate standard deviations (n = 3).

oropharyngeal swab samples, which can distinguish patients from healthy individuals, confirming the potential in clinical application. By virtue of being low-cost and user-friendly, the proposed biosensor may provide a new option for COVID-19 diagnosis to help control the outbreak and spread of the pandemic.

CRediT authorship contribution statement

Ying Deng: Conceptualization, Methodology, Validation, Writing – review & editing. **Ying Peng:** Writing – original draft, Investigation, Validation. **Lei Wang:** Investigation, Software. **Minghui Wang:** Investigation, Visualization. **Tianci Zhou:** Investigation, Data curation. **Jinlong Li:** Data curation, Data Collection, Data curation. **Jie Yang:** Data curation, Validation. **Genxi Li:** Writing – review & editing, Supervision.

Declaration of competing interest

The authors declare that they have no known competing financial interests or personal relationships that could have appeared to influence the work reported in this paper.

Acknowledgements

This work was supported by the National Natural Science Foundation of China (Grant No. 81772593) and the Fundamental Research Funds for the Central Universities (Grant No. 14380163).

Appendix A. Supplementary data

Supplementary data to this article can be found online at https://doi.org/10.1016/j.aca.2022.339846.

References

[1] B. Hu, H. Guo, P. Zhou, Z.-L. Shi, Characteristics of SARS-CoV-2 and COVID-19, Nat. Rev. Microbiol. 19 (3) (2021) 141–154.
[2] L. Shi, L. Wang, X. Ma, X. Fang, L. Xiang, Y. Yi, J. Li, Z. Luo, G. Li, Aptamer-functionalized nanochannels for one-step detection of SARS-CoV-2 in samples from COVID-19 patients, Anal. Chem. 93 (49) (2021) 16646–16654.
[3] P. Rai, B.K. Kumar, V.K. Deekshit, I. Karunasagar, I. Karunasagar, Detection technologies and recent developments in the diagnosis of COVID-19 infection, Appl Microbiol Biot 105 (2) (2021) 441–455.
[4] Y. Peng, Y. Pan, Z. Sun, J. Li, Y. Yi, J. Yang, G. Li, An electrochemical biosensor for sensitive analysis of the SARS-CoV-2 RNA, Biosens. Bioelectron. 186 (2021) 113309.
[5] W. Feng, A.M. Newbigging, C. Le, B. Pang, H. Peng, Y. Cao, J. Wu, G. Abbas, J. Song, D.-B. Wang, M. Cui, J. Tao, D.L. Tyrrell, X.-E. Zhang, H. Zhang, X.C. Le, Molecular diagnosis of COVID-19: challenges and research needs, Anal. Chem. 92 (15) (2020) 10196–10209.
[6] V.M. Corman, O. Landt, M. Kaiser, R. Molenkamp, A. Meijer, D.K. Chu, T. Bleicker, S. Brünink, J. Schneider, M.L. Schmidt, D.G. Mulders, B.L. Haagmans, B. van der Veer, S. van den Brink, L. Wijsman, G. Goderski, J.-L. Romette, J. Ellis, M. Zambon, M. Peiris, H. Goossens, C. Reusken, M.P. Koopmans, C. Drosten, Detection of 2019 novel coronavirus (2019-nCoV) by real-time RT-PCR, Euro Surveill. 25 (3) (2020) 2000045.
[7] M. Mohammadniaei, M. Zhang, J. Ashley, U.B. Christensen, L.J. Friis-Hansen, R. Gregersen, J.G. Lisby, T.L. Benfield, F.E. Nielsen, J. Henning Rasmussen, E. B. Pedersen, A.C.R. Olinger, L.T. Kolding, M. Naseri, T. Zheng, W. Wang, J. Gorodkin, Y. Sun, A non-enzymatic, isothermal strand displacement and amplification assay for rapid detection of SARS-CoV-2 RNA, Nat. Commun. 12 (1) (2021) 5089.

[8] S. Suleman, S.K. Shukla, N. Malhotra, S.D. Bukkitgar, N.P. Shetti, R. Pilloton, J. Narang, Y. Nee Tan, T.M. Aminabhavi, Point of care detection of COVID-19: advancement in biosensing and diagnostic methods, Chem. Eng. J. 414 (2021) 128759.
[9] T. Ai, Z. Yang, H. Hou, C. Zhan, C. Chen, W. Lv, Q. Tao, Z. Sun, L. Xia, Correlation of chest CT and RT-PCR testing for coronavirus disease 2019 (COVID-19) in China: a report of 1014 cases, Radiology 296 (2) (2020) E32–e40.
[10] W.J. Wiersinga, A. Rhodes, A.C. Cheng, S.J. Peacock, H.C. Prescott, Pathophysiology, transmission, diagnosis, and treatment of coronavirus disease 2019 (COVID-19): a review, JAMA 324 (8) (2020) 782–793.
[11] J. Moon, H.J. Kwon, D. Yong, I.C. Lee, H. Kim, H. Kang, E.K. Lim, K.S. Lee, J. Jung, H.G. Park, T. Kang, Colorimetricdetection of SARS-CoV-2 and drug-resistant pH1N1 using CRISPR/dCas9, ACS Sens. 5 (12) (2020) 4017–4026.
[12] M.A. Lalli, J.S. Langmade, X. Chen, C.C. Fronick, C.S. Sawyer, L.C. Burcea, M. N. Wilkinson, R.S. Fulton, M. Heinz, W.J. Buchser, R.D. Head, R.D. Mitra, J. Milbrandt, Rapid and extraction-free detection of SARS-CoV-2 from saliva by colorimetric reverse-transcription loop-mediated isothermal amplification, Clin. Chem. 67 (2) (2021) 415–424.
[13] J. Arizti-Sanz, C.A. Freije, A.C. Stanton, B.A. Petros, C.K. Boehm, S. Siddiqui, B. M. Shaw, G. Adams, T.F. Kosoko-Thoroddsen, M.E. Kemball, J.N. Uwanibe, F. V. Ajogbasile, P.E. Eromon, R. Gross, L. Wronka, K. Caviness, L.E. Hensley, N. H. Bergman, B.L. MacInnis, C.T. Happi, J.E. Lemieux, P.C. Sabeti, C. Myhrvold, Streamlined inactivation, amplification, and Cas13-based detection of SARS-CoV-2, Nat. Commun. 11 (1) (2020) 5921.
[14] B. Ning, T. Yu, S. Zhang, Z. Huang, D. Tian, Z. Lin, A. Niu, N. Golden, K. Hensley, B. Threeton, C.J. Lyon, X.M. Yin, C.J. Roy, N.S. Saba, J. Rappaport, Q. Wei, T. Y. Hu, A smartphone-read ultrasensitive and quantitative saliva test for COVID-19, Sci. Adv. 7 (2) (2021).
[15] G. Qiu, Z. Gai, Y. Tao, J. Schmitt, G.A. Kullak-Ublick, J. Wang, Dual-functional plasmonic photothermal biosensors for highly accurate severe acute respiratory syndrome coronavirus 2 detection, ACS Nano 14 (5) (2020) 5268–5277.
[16] J. Lukose, S. Chidangil, S.D. George, Optical technologies for the detection of viruses like COVID-19: progress and prospects, Biosens. Bioelectron. 178 (2021) 113004.
[17] S.D. Bukkitgar, N.P. Shetti, T.M. Aminabhavi, Electrochemical investigations for COVID-19 detection-A comparison with other viral detection methods, Chem. Eng. J. 420 (2021) 127575.
[18] J. Su, Y. Ke, N. Maboyi, X. Zhi, S. Yan, F. Li, B. Zhao, X. Jia, S. Song, X. Ding, CRISPR/Cas12a Powered DNA Framework-supported electrochemical biosensing platform for ultrasensitive nucleic acid analysis, Small Methods 5 (12) (2021) 2100935.
[19] Y. Dai, R.A. Somoza, L. Wang, J.F. Welter, Y. Li, A.I. Caplan, C.C. Liu, Exploring the trans-cleavage activity of CRISPR-Cas12a (cpf1) for the development of a universal electrochemical biosensor, Angew Chem. Int. Ed. Engl. 58 (48) (2019) 17399–17405.
[20] J. Kudr, P. Michalek, L. Ilieva, V. Adam, O. Zitka, COVID-19: a challenge for electrochemical biosensors, Trac. Trends Anal. Chem. 136 (2021) 116192.
[21] Z. Song, Y. Ma, M. Chen, A. Ambrosi, C. Ding, X. Luo, Electrochemical biosensor with enhanced antifouling capability for COVID-19 nucleic acid detection in complex biological media, Anal. Chem. 93 (14) (2021) 5963–5971.
[22] X. Lu, H. Lee Yu, H. Lin, Y. Cao, I.M. Hsing, Rapid and highly specific detection of communicable pathogens using one-pot loop probe-mediated isothermal amplification (oLAMP), Sensor. Actuator. B Chem. 357 (2022) 131385.
[23] A.P.K.K. Karunanayake Mudiyanselage, Q. Yu, M.A. Leon-Duque, B. Zhao, R. Wu, M. You, Genetically encoded catalytic hairpin assembly for sensitive RNA imaging in live cells, J. Am. Chem. Soc. 140 (28) (2018) 8739–8745.
[24] J. Liu, Y. Zhang, H. Xie, L. Zhao, L. Zheng, H. Ye, Applications of catalytic hairpin assembly reaction in biosensing, Small 15 (42) (2019) 1902989.
[25] F. Ma, Q. Zhang, C.-y. Zhang, Catalytic Self-assembly of quantum-dot-based microrna nanosensor directed by toehold-mediated strand displacement cascade, Nano Lett. 19 (9) (2019) 6370–6376.
[26] B. Li, Y. Liu, Y. Liu, T. Tian, B. Yang, X. Huang, J. Liu, B. Liu, Construction of dual-color probes with target-triggered signal amplification for in situ single-molecule imaging of MicroRNA, ACS Nano 14 (7) (2020) 8116–8125.
[27] H. Wang, H. Wang, I. Willner, F. Wang, High-performance biosensing based on autonomous enzyme-free DNA circuits, Top. Curr. Chem. 378 (1) (2020) 20.
[28] Y.-C. Du, S.-Y. Wang, Y.-X. Wang, J.-Y. Ma, D.-X. Wang, A.-N. Tang, D.-M. Kong, Terminal deoxynucleotidyl transferase combined CRISPR-Cas12a amplification strategy for ultrasensitive detection of uracil-DNA glycosylase with zero background, Biosens. Bioelectron. 171 (2021) 112734.
[29] L. Wang, Y. Deng, J. Wei, Y. Huang, Z. Wang, G. Li, Spherical nucleic acids-based cascade signal amplification for highly sensitive detection of exosomes, Biosens. Bioelectron. 191 (2021) 113465.
[30] K. Zhang, Z. Fan, Y. Ding, M. Xie, A pH-engineering regenerative DNA tetrahedron ECL biosensor for the assay of SARS-CoV-2 RdRp gene based on CRISPR/Cas12a trans-activity, Chem. Eng. J. 429 (2022) 132472.
[31] P. Zhou, X.-L. Yang, X.-G. Wang, B. Hu, L. Zhang, W. Zhang, H.-R. Si, Y. Zhu, B. Li, C.-L. Huang, H.-D. Chen, J. Chen, Y. Luo, H. Guo, R.-D. Jiang, M.-Q. Liu, Y. Chen, X.-R. Shen, X. Wang, X.-S. Zheng, K. Zhao, Q.-J. Chen, F. Deng, L.-L. Liu, B. Yan, F.-X. Zhan, Y.-Y. Wang, G.-F. Xiao, Z.-L. Shi, A pneumonia outbreak associated with a new coronavirus of probable bat origin, Nature 579 (7798) (2020) 270–273.
[32] S. Barthel, S. Palluk, N.J. Hillson, J.D. Keasling, D.H. Arlow, Enhancing terminal deoxynucleotidyl transferase activity on substrates with 3' terminal structures for enzymatic de novo DNA synthesis, Genes 11 (1) (2020) 102.